

● *Original Contribution*

OPTIMAL DETECTION OF BLOOD-BRAIN BARRIER DEFECTS WITH Gd-DTPA MRI—THE INFLUENCES OF DELAYED IMAGING AND OPTIMISED REPETITION TIME

PAUL S. TOFTS

NMR Research Unit, Institute of Neurology, National Hospital for Neurology and Neurosurgery, London WC1N 3BG, UK

A computer simulation of Gd-DTPA enhancement in blood–brain barrier defects was used to find the tissue concentration as a function of time after bolus injection for a variety of lesion permeability and leakage space values. High permeability lesions start to decay less than 10 min after injection; while low permeability lesions may not reach their maximum concentration until at least 2 h after injection. The minimum detectable permeability was calculated for a range of leakage space values. For a leakage space of 0.1, 2 h after a standard 0.1 mmol/kg injection a permeability surface area product as low as 0.0005 min⁻¹ still gives detectable enhancement, while 6 min after injection the permeability must be at least six times higher to give detectable enhancement. The simulation shows that the effect of triple dose compared to standard dose cannot be found using cumulative dose experiments where the triple dose is fractionated over a period of 10–30 min.

Keywords: Gd-DTPA; Permeability; Triple dose; Delayed scanning.

INTRODUCTION

With the advent of nonionic Gd-containing contrast media, there is currently much interest in studying the use of increased doses (double or triple the conventional 0.1 mmol/kg) to improve the chance of detecting blood–brain barrier lesions.^{1–9,28} Imaging usually takes place within 3–5 min of injection; however, many lesions continue to enhance after that time, and some groups have looked for an increased yield of particular types of lesion by delaying the imaging time.^{6,10,11} It is, therefore, important to have a conceptual framework within which to study the effect of delayed imaging.

An approach to optimising the chance of detecting blood–brain barrier lesions using T₁-weighted imaging after injection of Gd-DTPA is presented. It is based on a compartmental model of Gd-DTPA distribution,¹² and consists of three parts. First, the optimum time between injection and imaging is investigated. Second, the imaging parameters TR (the repetition time) and NEX (the number of excitations) are optimised for a given total examination time, for both spin echo and

gradient echo sequences. Third, the minimum detectable permeability is estimated for a range of lesion leakage space values and times after injection. The assessment of triple dose injections using a fractionated dose regime is found to be generally invalid. A preliminary account of this work has already been presented.¹³

MATERIALS AND METHODS

The model of Gd-DTPA distribution and signal enhancement used in this simulation was first applied to the estimation of permeability and leakage space in Multiple Sclerosis lesions.¹² Later, it was validated in blood–retina lesions.¹⁴ Permeability measured using the MRI signal enhancement in the vitreous humour was in agreement with that measured directly from the amount of Gd-DTPA that had leaked into the vitreous humour. Recently, the model has also been used to estimate permeability in breast tumours.¹⁵ It consists of a plasma compartment, into which a bolus dose D mmol/kg of Gd-DTPA tracer is injected at time $t = 0$, an extracellular compartment that is in good contact with the plasma, a lesion connected to the plasma by

a leak, and renal extraction of tracer from the plasma. The lesion is characterised by its transfer constant k (units min^{-1}), or PS (Permeability Surface area) product per unit volume, loosely referred to as its 'permeability,' and by its leakage space v_1 , which is the proportion of the lesion tissue volume that is accessible to Gd-DTPA ($0 \leq v_1 \leq 1$). The leakage space is probably the extracellular space.

The plasma concentration decays biexponentially after the bolus injection, in agreement with measurements.¹⁶

$$C_p(t) = D \sum_{i=1}^2 a_i e^{-m_i t} \quad (1)$$

where $i = 1$ describes the early mixing phase between plasma and extracellular water, and $i = 2$ describes the later renal excretion phase. In humans the data of Weinmann et al.,¹⁶ fit $a_1 = 3.99 \text{ kg/liter}$, $a_2 = 4.78 \text{ kg/liter}$, $m_1 = 0.144 \text{ min}^{-1}$, $m_2 = 0.0111 \text{ min}^{-1}$.¹² The resulting tissue concentration is the sum of exponentials with three time constants:¹²

$$C_t(t) = D k \sum_{i=1}^2 a_i (e^{-m_3 t} - e^{-m_i t}) / (m_i - m_3) \quad (2)$$

where $m_3 = k/v_1$.

In this simulation the lesion concentration was calculated for a variety of values of permeability; the range went from the lowest permeability lesion that appeared detectable ($k = 0.001 \text{ min}^{-1}$) up to a value 100 times higher. The latter ($k = 0.1 \text{ min}^{-1}$) is high enough to keep the concentration in the leakage space in good equilibrium with that in the plasma. Two extreme values of leakage space v_1 were used, corresponding to the lowest ($v_1 = 0.1$) and highest ($v_1 = 0.8$) values likely to be found in real lesions, although smaller values were also investigated. The concentration in the plasma, and also in the lesion, is directly proportional to the injected dose.

The increase in signal caused by a particular concentration of Gd-DTPA has been modelled.¹² For a T_1 -weighted spin echo (with negligibly short echo time) the signal is

$$S_{SE} = S_0 (1 - e^{-\text{TR}(T_1^{-1} + R_1 C)}) \quad (3)$$

where S_0 is the relaxed signal (i.e., at long TR), T_1 is the T_1 before injection of Gd-DTPA, R_1 is the relaxivity of Gd-DTPA ($4.5 \text{ s}^{-1} \text{ mM}^{-1}$ at 1.5T¹⁷), and C is the tissue concentration of Gd-DTPA in mM. The increase in signal caused by a small concentration of Gd-DTPA is¹⁸

$$\Delta S = S_0 R_1 T_k C \quad (4)$$

where T_k describes the T_1 -weighting of the sequence:

$$T_k = \frac{1}{S_0} \left(\frac{\partial S}{\partial (1/T_1)} \right)_{C=0} = \frac{1}{S_0 R_1} \left(\frac{\partial S}{\partial C} \right)_{C=0} \quad (5)$$

For a spin echo [Eq. (3)],

$$T_{k(SE)} = \text{TR} e^{-\text{TR}/T_1} \quad (6)$$

The signal from a spoiled gradient echo sequence¹⁹ is:

$$S_{GE} = S_0 \frac{(1 - e^{-\text{TR}(T_1^{-1} + R_1 C)}) \sin \theta}{1 - \cos \theta e^{-\text{TR}(T_1^{-1} + R_1 C)}} \quad (7)$$

where θ is the tip angle, and the T_1 -weighting is given by

$$T_{k(GE)} = \frac{\text{TR} e^{-\text{TR}/T_1} \sin \theta (1 - \cos \theta)}{(1 - \cos \theta e^{-\text{TR}/T_1})^2} \quad (8)$$

Assuming that to see leakage the signal must increase by at least three times the rms noise level, then the minimum detectable concentration of Gd-DTPA is [from Eq. (4)]

$$C_{\min} = \frac{3}{\text{SNR}_0 R_1 T_k \sqrt{\text{NEX}}} \quad (9)$$

where NEX is the number of excitations (averages) used to collect the image, and SNR_0 is the signal-to-noise ratio in a single-average relaxed SE image (NEX = 1). For a given examination time T_{ex} that is available for imaging, the number of excitations NEX that can be used is the nearest integer to $T_{\text{ex}}/(N_{\text{pe}} \text{TR})$, where N_{pe} is the number of phase encoding steps. Using Eqs. (9), (6), and (8), the minimum detectable concentration of Gd-DTPA was calculated as a function of TR, for a given examination time. The T_1 of white matter at 1.5T was used (600 ms).²⁰ For gradient echo sequences the optimum TR at each tip angle was also found, and the sensitivity of the sequence found by comparing the minimum detectable concentration of Gd with that obtained with the optimised spin echo sequence.

The dependence of C_{\min} on TR was also examined analytically for the spin echo sequence. NEX was made a continuous variable (this is a reasonable approximation when NEX is large). Using Eqs. (9) and (6), setting $\text{NEX} = T_{\text{ex}}/(N_{\text{pe}} \text{TR})$, and minimising C_{\min} with respect to TR, the optimum repetition time is:

$$TR^{\text{opt(SE)}} = T_{10}/2 \quad (10)$$

and the optimised minimum detectable concentration is then

$$C_{\text{min}}^{\text{opt(SE)}} = \frac{7.0}{\text{SNR}_0 R_1} \left(\frac{N_{\text{pe}}}{T_{\text{ex}} T_{10}} \right)^{1/2} \quad (11)$$

At sufficiently high concentrations of Gd-DTPA the spins relax completely between pulses, so that the sequence is no longer T_1 -weighted. This effect was studied for the SE sequence by plotting signal vs. Gd concentration, using Eq. (3), for a range of repetition times.

The minimum permeability that could be detected was calculated for a range of lesion leakage spaces ($v_l = 0.02$ – 0.80) and times after injection for the optimised spin echo sequence, at both the standard ‘single’ dose (0.1 mmol/kg) and ‘triple’ dose (0.3 mmol/kg). This was carried out by increasing the permeability from zero, at a fixed leakage space and time, until the tissue concentration [Eq. (2)] reached the optimised minimum detectable concentration [Eq. (11)].

RESULTS

The tissue concentration of Gd-DTPA achieved as a function of time is shown in Fig. 1 for a standard (single) dose. At the low value of leakage space ($v_l = 0.1$, Fig. 1a), the high permeability lesion reaches maximum concentration almost instantly (within the plasma mixing time of less than 1 min) and then declines. However, lower permeability lesions take longer to reach their maximum concentration, and the $k = 0.001 \text{ min}^{-1}$ lesion, which is just at the limit of detection, only reaches its maximum concentration about 80 min after injection. With a higher leakage space ($v_l = 0.8$, Fig. 1b) the times to peak concentration are delayed (because it takes longer to fill the larger leakage space), and the tissue concentrations achieved are higher (because a higher proportion of the tissue is accessible to Gd-DTPA). Even after 2 h the concentration in the lower permeability lesion is still increasing. Leakage spaces smaller than 0.1 (i.e., $v_l < 0.1$) have curves the same shape as shown in Fig. 1a, but scaled down in proportion to v_l . Lesions that occupy less than a voxel will also be scaled down in proportion to their partial volume.

The minimum detectable concentration of Gd-DTPA, as a function of repetition time, is shown in Fig. 2 for white matter. The discontinuities arise because the number of excitations NEX is quantised to be integer. The curves of $C_{\text{min}}^{\text{opt}}$ vs. TR are broad, and any value of TR between 0.5 and 1.7 times the opti-

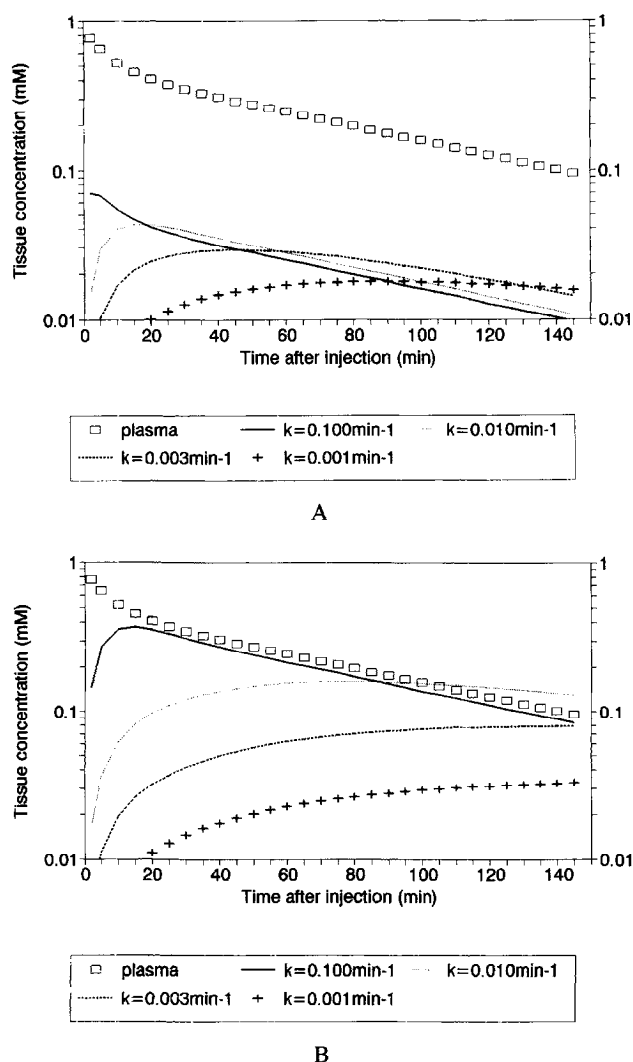


Fig. 1. The concentration of Gd-DTPA in the plasma and in white matter lesions of various permeabilities k (min^{-1}), after a bolus dose of 0.1 mmol/kg of Gd-DTPA. (a) Lesion leakage space $v_l = 0.1$; (b) $v_l = 0.8$.

um can be used without increasing the minimum detectable concentration by more than 10%, for both the spin echo and gradient echo sequences [provided the total exam time T_{ex} is unchanged; see Eq. (11)]. For a spin echo, repetition times in the range 150–500 ms are optimum, and any convenient value in this range can be used, depending on the number of slices required. For a signal-to-noise ratio of 100 in the relaxed image, and 192 phase encoding gradients, the minimum detectable concentration of Gd-DTPA is 0.011 mM for an examination time of 10 min. The analytic solution [Eqs. (10) and (11)] confirms the values of optimum TR and C_{min} obtained from Fig. 2. This minimum detectable value for the optimised sequence (0.011 mM), lies near the bottom of Figs. 1A and B, and, therefore, any combination of permeability,

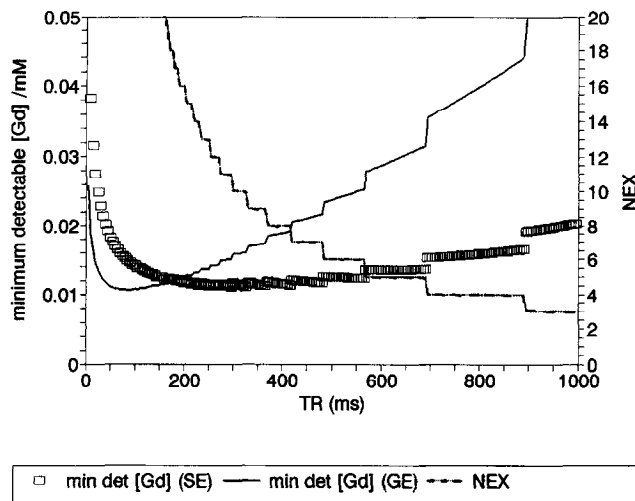


Fig. 2. The minimum detectable concentration of Gd-DTPA in white matter ($T_{10} = 600$ ms at 1.5 T) as a function of repetition time for spin echo (SE) and gradient echo (GE; $\theta = 50^\circ$) sequences (left hand axis). Also shown are the number of excitations NEX, decreasing as TR is increased (right hand axis). The total examination time is kept approximately constant at 10 min. The signal-to-noise ratio in the relaxed spin echo image (NEX = 1) is 100; 192 phase encodes were used.

leakage space, and time after injection that appears in the figures gives sufficient enhancement to be detectable. Increasing the dose simply increases the tissue concentration in direct proportion to the dose.¹² Hence, a dose of 0.3 mmol/kg raises all the curves in Fig. 1 by a factor of 3, and allows lesions with lower permeability to be detected.

Optimal tip angles for gradient echo sequences with various repetition times are shown in Fig. 3. The range by which the tip angle can vary without decreasing the sensitivity by more than 10% is also shown. The minimum detectable concentration is between 93 and 100% of that for an optimised spin echo sequence.

The behaviour of the spin echo sequence at high concentrations is shown in Fig. 4 for white matter ($T_{10} = 600$ ms). Concentration values up to 1 mM, exceeding that found in the plasma (see Fig. 1) were investigated. The signal increase has been divided by the noise after NEX averages (assuming NEX is a continuous variable). At low concentrations, the curve with the greatest slope (i.e., the highest sensitivity) is that for TR = 300 ms, as expected. At higher concentrations all the curves still show reasonable T_1 -weighting, although those with lowest TR plateau out last, as expected. Thus the repetition time that is optimum for detection of low concentrations (i.e., TR = 300 ms in Fig. 2) still performs well at high concentrations, with little loss of T_1 -weighting.

The minimum permeability leakage that can be de-

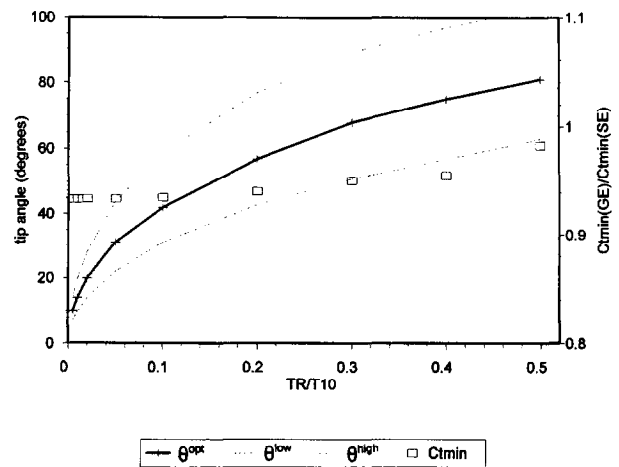


Fig. 3. The optimum tip angle (θ^{opt} ; left-hand axis) for gradient echo sequences with a range of repetition times TR, expressed as a fraction of T_{10} (the T_1 in the tissue before injection of Gd-DTPA). The tip angle can be altered within the range θ^{low} to θ^{high} without increasing the minimum detectable concentration of Gd-DTPA by more than 10%. The minimum detectable concentration of Gd-DTPA at this optimised repetition time, Cmin(GE), is shown as a fraction of Cmin(SE), the minimum detectable concentration for an optimised spin echo sequence (right-hand axis).

tected is shown in Fig. 5, for standard and triple dose. Lesions with small leakage space ($v_l = 0.02$), or those that occupy a small fraction of a voxel, only attain a low tissue concentration of Gd-DTPA. For these lesions the highest concentrations are achieved with a high permeability, and these can be seen soon after

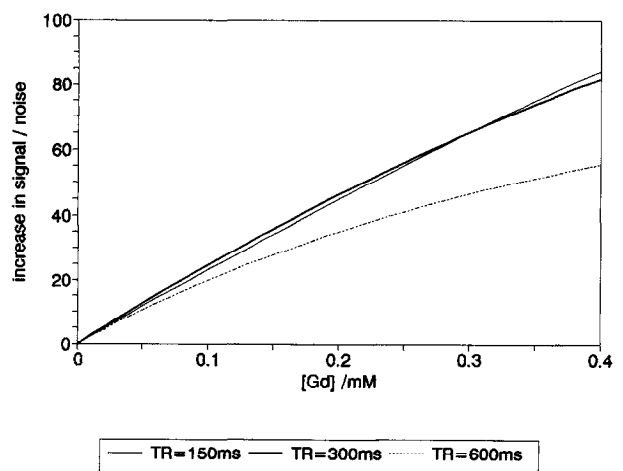


Fig. 4. The behaviour of spin echo sequences at high concentrations of Gd-DTPA in white matter ($T_{10} = 600$ ms at 1.5 T). The optimal TR (300 ms) has the greatest slope, and maintains reasonable linearity up to the highest Gd-DTPA concentrations found in lesions (0.4 mM, see Fig. 1b). Total examination time is 10 min. The signal-to-noise ratio in the relaxed spin echo image (NEX = 1) is 100; 192 phase encodes were used.

injection (because these lesions are in good contact with the plasma, their concentration vs. time curves have the same shape as those for the plasma; see also Fig. 1). After 10 min this lesion ($v_l = 0.02$) is undetectable with a standard dose, regardless of how great its permeability; however, triple dose enables it to be seen even with a relatively low permeability, provided delayed imaging is used. As the leakage space is increased, higher concentrations can be achieved, provided time is allowed for them to fill up (see also Fig. 1), and lower permeabilities can be detected. For a very watery lesion ($v_l = 0.80$, in Fig. 5) sensitivity is still improving after 2 h. Because the permeability is low, the concentration in the leakage space is still below that in the plasma, and the direction of flow is still into the lesion.

DISCUSSION

Depending on the nature of a lesion (i.e., its permeability and leakage space), this simulation shows that the optimum time to detect it may be immediately after injection (as for the vascular or high permeability tumours), or it may be much later (up to 1 h or more, for low permeability lesions). This conclusion is sup-

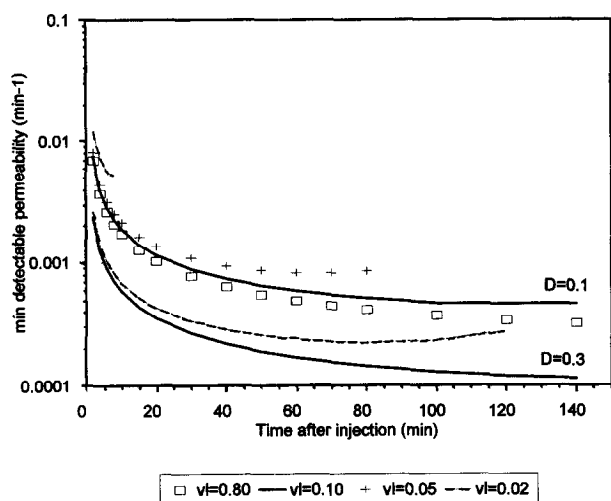


Fig. 5. The minimum detectable permeability for a range of lesion leakage space values (v_l) and times after injection. Bolus doses of 0.1 mmol/kg of Gd-DTPA (upper data: $v_l = 0.80, 0.10, 0.05, 0.02$) and 0.3 mmol/kg (lower data: $v_l = 0.10, 0.02$) are shown. With a standard 0.1 mmol/kg dose lesions with small leakage space (or those occupying a small fraction of a voxel) can only be detected if they have high permeability, and if they are imaged early after injection. Lesions with large leakage space can be detected even if they have low permeability, provided delayed imaging is used. The signal-to-noise ratio in the relaxed spin echo image (NEX = 1) was 100. One hundred ninety-two phase encodes, a TR of 300 ms, and 10 NEX (averages) were used. The total examination time was 10 min.

ported by the work of Kermod et al.,²¹ who studied the time course of enhancement in 102 enhancing multiple sclerosis lesions. They found that maximum signal intensity was reached between 4 and 120 min after injection, with a great majority of lesions reaching it around the mean time of 29 min. Many smaller and uniformly enhancing lesions had disappeared by 80 min, while larger ring lesions remained bright 5 h after injection. At 5 min the concentration of Gd-DTPA in multiple sclerosis lesions may be only 30% of its maximum value.¹² The failure to detect leakage in some Multiple Sclerosis and HIV positive patients may be caused by a low permeability and, hence, the long time required to reach maximum enhancement. Increasing the dose will enable lesions with still lower permeability or leakage space to be seen; its benefit is in addition to any obtained from delayed imaging (see Fig. 5).

Delayed imaging need not consume more imaging time. Two approaches are possible. First, if only low permeability lesions are sought, the subject is injected and then imaged about 60 min later. Second, if lesions with a wide range of permeabilities are sought, the imaging takes place immediately after injection; the subject is removed while another study takes place; then the subject is replaced for delayed imaging.

The gradient echo sequence is able to detect the same concentration as the spin echo, by using a shorter TR (see Fig. 2). Spin echoes are usually to be preferred to 2D gradient echo sequences, because the longer TR allows more slices to be collected, and the signal is not diminished by T_2^* losses. With a 2D gradient echo sequence the number of slices may be increased by using several acquisition blocks, but the sensitivity will be reduced because any particular slice is not being interrogated for the whole examination time, as has been assumed in this simulation. However, 3D gradient echoes may have useful advantages over the spin echo sequence if good 3D resolution is required (e.g., for spatial registration in software, see below), or if imaging the vitreous humour ($T_1 = 4$ s), when the optimum TR with a spin echo (i.e., 2 s) could require a prohibitively long exam time. For example a $128 \times 128 \times 256$ 3D acquisition in white matter with TR = 30 ms would take 8 min and the optimum tip angle would be 31° (range 22 to 44°). A $128 \times 128 \times 256$ 3D acquisition in the vitreous humor with TR = 40 ms would take 11 min and the optimum tip angle would be 14° (range 10 to 20°). The reduction in slice thickness will give a signal-to-noise disadvantage, which could be recovered by reformatting into thicker slices before viewing. Gradient echo sequences may also suffer a reduction in sensitivity, by a factor of probably no more than $\sqrt{2}$, arising from the use of fractional echo and increased bandwidth during acquisition.

The ability to detect small concentrations of Gd-

DTPA may be improved, particularly if the lesion is hypo-intense in the preinjection T_1 -weighted image, by subtracting the preinjection image, where such image manipulation facilities are available.²² This is collected with the same parameters as the postinjection image. The images must be registered, preferably to within less than a pixel. If the subject is not removed from the imager between the pre and postinjection images, then injection can be via a catheter, and the subject can be assisted in keeping still with a nose ring.²³ Alternatively, if the subject is removed between the pre- and postinjection images, then oblique pilots can be used to align each multislice image set with respect to internal landmarks.²⁴ In-plane movement can be corrected by movement of the images in the computer to achieve a better registration. If there is substantial out-of-plane movement, a 3D collection may be preferred, enabling the datasets to be accurately registered to within less than a pixel in all directions.²⁵ The preinjection image should not be allowed to contribute noise to the difference image; this can be achieved in two possible ways: first, by using sufficient number of averages (several times the number used in the postinjection image, if there is time). Second, by lightly smoothing the preinjection image (preferably with an edge-preserving algorithm). A further possible way of improving the sensitivity would be to measure the signal at several time points, if it were possible to keep the patient in the MR machine for long enough. The signal intensities could then be combined to provide a time-correlation measure that is more sensitive than that obtained from a single postinjection signal intensity value.²⁶

This analysis has focused on detecting Gd-DTPA in white matter at 1.5T. However, it is equally applicable to other tissues (e.g., the vitreous humour, where Gd-DTPA can be seen accompanying blood-retina barrier breakdown),¹⁴ and to other magnetic field strengths, provided the appropriate values of T_{10} and R_1 are used. For a spin echo sequence Eqs. (10) and (11) can be used to predict the optimal TR and minimum detectable concentration of Gd-DTPA. For white matter at 1.5T they predict an optimum TR of 300 ms and a minimum detectable concentration of 0.011 mM, in agreement with Fig. 2. For blood-retinal leakage, where $T_{10} = 4$ s, the optimal TR is 2 s. Other renally excreted Gd-labelled contrast agents have recently been introduced. The plasma concentration of these will follow the same form as for Gd-DTPA, and the above analysis is equally applicable.

The effect of increased dose of contrast agent compared to a standard dose has been studied using injections made within a few minutes of each other.^{1,2,4,5,7,8} In all of these studies there is an implicit assumption that the dose under study can be 'fractionated' into

subdoses, whose sum is equal to the dose under study, without altering the pattern of enhancement. Niendorf et al.¹ gave injections of 0.05, 0.05, and 0.1 mmol/kg, each separated by 15 min, to compare doses of 0.05, 0.1, and 0.2 mmol/kg. Schubeus et al.² gave two injections of 0.1 mmol/kg separated by 25 min to compare doses of 0.1 and 0.2 mmol/kg. Yuh et al.⁴ gave doses of 0.1 and 0.2 mmol/kg 30 min apart to compare the dose of 0.1 with a higher (unspecified) dose (the cumulative dose was 0.3 mmol/kg). Runge et al.⁵ gave doses of 0.1 and 0.2 mmol/kg 30 min apart to compare doses of 0.1 and 0.3 mmol/kg. Lee et al.⁷ gave injections of 0.05, 0.05, and 0.1 mmol/kg, each separated by 10 min, to compare doses of 0.05, 0.1, and 0.2 mmol/kg. Vogl et al.⁸ gave doses of 0.1 and 0.2 mmol/kg 10 min apart to compare doses of 0.1 and 0.3 mmol/kg. The signal enhancement arising from the two individual doses is clearly different from that arising from one combined dose because the effect of a particular dose on the signal enhancement depends on how long before the image data acquisition the injection was given. For high permeability lesions (see Fig. 1), where the concentration arising from the first dose is decaying away rapidly in the first few minutes, the total enhancement arising from the cumulative doses will be less than if the same dose had been given as a single bolus. Conversely, for low permeability lesions the total enhancement will be greater than if the cumulative dose had been given as a single bolus, because the earlier doses will have the benefit of delayed imaging. An example of this is given in Fig. 6, where the effect of fractionation, 6 min after comple-

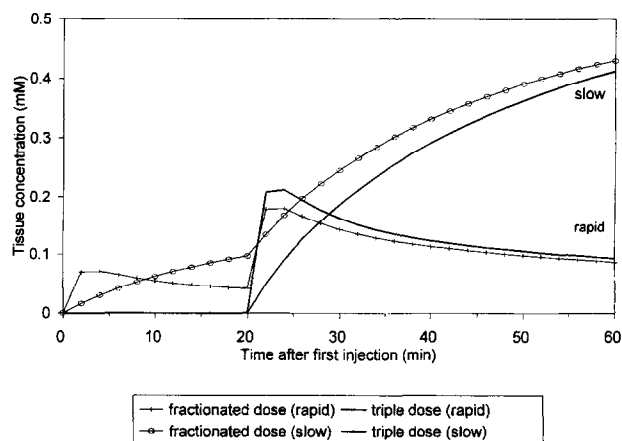


Fig. 6. The effect of dose fractionation. A triple dose given as a single bolus at time 20 min produces the tissue concentrations shown by the solid lines for a rapidly enhancing lesion ($k = 0.1 \text{ min}^{-1}$, $v_1 = 0.1$) and a slowly enhancing lesion ($k = 0.01 \text{ min}^{-1}$, $v_1 = 0.8$). If the dose is fractionated so that a single dose is given at time zero followed by a double dose at 20 min, the tissue concentration (symbols) is lowered for the rapid lesion and raised for the slow lesion.

tion of a triple dose, is to reduce the concentration by 14% in a rapidly enhancing lesion and to increase it by 56% in a slowly enhancing lesion. Thus cumulative dose studies as a way of investigating the benefits of increased single boluses are fundamentally flawed. In addition the use of two closely timed doses prevents the benefits of delayed imaging of these doses from being evaluated.

Single and triple dose can only be realistically compared by injecting on different days and by using a range of delays between injection and imaging to see whether any benefits from increased dose can also be obtained by using standard dose with delayed imaging. Yuh et al.³ looked at a range of doses, though never in the same patient. Hausteine et al.⁶ gave doses of either 0.1 or 0.3 mmol/kg to paired patients; this method overcomes the problems of the cumulative dose method, but introduces the large interpatient variability that may overwhelm the effects of the increased dose, and in this study a large number (199) of patients were used. The most sound investigation to date is that of Filippi et al.,^{9,28} who studied doses of 0.1 and 0.3 mmol/kg in the same patients 6–24 h apart and found more enhancing lesions in multiple sclerosis with the increased dose.

In this simulation it has been assumed that the T_1 of the leaking white matter before injection of Gd-DTPA (i.e., T_{10}) is not significantly raised compared to the normal value of 600 ms. From this, an optimum TR of 300 ms was predicted. Because blood–brain barrier leakage usually precedes other pathologic changes, this is a reasonable assumption. If T_{10} is higher than the normal value, there will be two consequences. First, the minimum detectable concentration of Gd-DTPA [Eq. (11)] will be reduced (i.e., the optimised sequence will be more sensitive). Second, the optimum TR is increased [Eq. (10)]. Given that minimum in the C_t^{opt} vs. TR curve is shallow (Fig. 2), and that TR can be increased to 1.7 TR^{opt} without losing more than 10% sensitivity (see Results section), the TR could be increased to 500 ms. This would then cover T_{10} values in the range 600–1000 ms. Two more simplifying assumptions are implicit in the model.¹² First, the plasma volume is assumed to be negligibly small, so that enhancement arising from Gd-DTPA in the capillaries can be neglected. In normal white matter blood is thought to occupy about 2–4% of the total volume, which is much smaller than the extracellular space (at least 16%), and it is known that no signal enhancement is seen in normal white matter. This assumption is then justified in pathologies where the vasculature is not enlarged, such as multiple sclerosis. In tumours with an enlarged vasculature there would be rapid enhancement following the time course of the plasma curve (similar to the $k = 0.1 \text{ min}^{-1}$ curve in Fig. 1a); this will be in addition to the effect of any leakage into the extracellular space, which will have a time course

appropriate to the permeability and leakage space of the defect (Fig. 1a and b). Second, the permeabilities in both directions (i.e., from plasma to extracellular space, and from extracellular space back to plasma) have been assumed equal. This is reasonable for any passive form of transport that is driven by the concentration difference across the capillary wall, such as diffusion, and in the absence of evidence to the contrary this simplest situation has been used. In tumours the transfer constants in each direction (k_1 and k_2) may be unequal;²⁷ however, attempts to determine them directly are unsuccessful, because k_1 cannot be determined directly, but only as part of the product $k_1 v_1$.²⁷

In conclusion, this simulation has shown that:

1. Small leakage space lesions may only be detectable within 10 min of injection.
2. Large leakage space lesions are more easily detected with imaging delayed up to 2 h, when permeabilities as low as 0.0005 min^{-1} produce detectable enhancement with a standard 0.1 mmol/kg dose.
3. Increasing the dose enables lesions with lower permeabilities and smaller leakage spaces to be detected.
4. Comparison of single and triple dose sensitivity in detecting lesions cannot be made using the cumulative dose procedure, where the triple dose is fractionated.
5. Spin echo sequences are most sensitive with a TR equal to half the T_1 of the unenhanced tissue (i.e., a TR about 300–500 ms for white matter).
6. Gradient echo sequences are at least as sensitive as spin echo sequences, provided an appropriate tip angle is used.

Acknowledgements—I am grateful to Dr. Gareth Barker for helpful discussions. The NMR Research Unit at Queen Square is generously supported by the Multiple Sclerosis Society of Great Britain and Northern Ireland.

REFERENCES

1. Niendorf, H.P.; Laniado, M.; Semmler, W.; Schorner, W.; Felix, R. Dose administration of gadolinium-DTPA in MR imaging of intracranial tumors. *AJNR* 8:803–815; 1987.
2. Schubeus, P.; Schorner, W.; Hausteine, J. Dosing of Gd-DTPA in MR imaging of intracranial tumors. *Magn. Reson. Med.* 22:249–254; 1991.
3. Yuh, W.T.C.; Fisher, D.J.; Engelken, J.D.; Greene, G.M.; Sato, Y.; Ryals, T.J.; Crain, M.R.; Ehrhardt, J.C. MR evaluation of CNS tumors: Dose comparison study with gadopentetate dimeglumine and gadoteridol. *Radiology* 180:485–491; 1991.
4. Yuh, W.T.C.; Engelken, J.D.; Muhonen, M.G.; Mayr, N.A.; Fisher, D.J.; Ehrhardt, J.C. Experience with high-dose Gadolinium MR imaging in the evaluation of brain metastases. *AJNR* 13:335–345; 1992.
5. Runge, V.M.; Kirsch, J.E.; Burke, V.J.; Price, A.C.; Nel-

- son, K.L.; Thomas, G.S.; Dean, B.L.; Lee, C. High-dose gadoteridol in MR imaging of intracranial neoplasms. *J. Magn. Reson. Imaging* 2:9–18; 1992.
6. Haustein, J.; Laniado, M.; Niendorf, H.-P.; Louton, T.; Beck, W.; Planitzer, J.; Schoffel, M.; Reiser, M.; Kaiser, W.; Schorner, W.; Hierholzer, J.; Traupe, H.; Hamm, B. Triple-dose vs. standard dose gadopentetate dimeglumine: A randomised study in 199 patients. *Radiology* 186:855–860; 1993.
 7. Lee, D.; Kucharczyk, W.; Farb, R.; McClarty, B.; Trudel, G.C. Evaluation of additive doses of magnevist (gadopentetate dimeglumine) as an MRI contrast agent in detection of cerebral lesions. San Francisco: Society of Magnetic Resonance 2nd annual meeting; 1994: p. 445.
 8. Vogl, T.J.; Friebe, C.E.; Mack, M.G.; Balzer, T.; Felix, R. MR evaluation of brain metastases: Comparison of standard and high-dose gadobutrol vs. standard dose Gd-DTPA. San Francisco: Society of Magnetic Resonance 2nd annual meeting; 1994: p. 548.
 9. Filippi, M.; Campi, A.; Martinelli, V.; Colombo, B.; Yousry, T.; Canal, N.; Scotti, G.; Comi, G. Comparison of triple dose vs. standard dose Gadolinium-DTPA for detection of MRI enhancing lesions in patients with primary progressive multiple sclerosis. *J. Neurol. Neurosurg. Psychol.* 59:540–544; 1995.
 10. Schorner, W.; Laniado, M.; Niendorf, H.P.; Schubert, C.; Felix, R. Time-dependent changes in image contrast in brain tumors after gadolinium-DTPA. *AJNR* 7:1013–1020; 1986.
 11. Davis, P.C.; Gokhale, K.A.; Joseph, G.J.; Peterman, S.B.; Adams, D.A.; Tindall, G.T.; Hudgins, P.A.; Hoffman, J.C. Pituitary adenoma: Correlation of half-dose gadolinium-enhanced MR imaging with surgical findings in 26 patients. *Radiology* 180:779–784; 1991.
 12. Tofts, P.S.; Kermode, A.G. Measurement of the Blood-Brain Barrier permeability and leakage space using dynamic MR imaging—1. Fundamental concepts. *Magn. Reson. Med.* 17:357–367; 1991
 13. Tofts, P.S. Optimal detection of blood–brain barrier defects with Gd-DTPA—The influence of delayed imaging and optimised repetition time. Nice, France: Society of Magnetic Resonance 3rd annual meeting; 1995: p. 1296.
 14. Berkowitz, B.A.; Tofts, P.S.; Sen, H.A.; Ando, N.; de Juan, E. Accurate and precise measurement of blood-retinal barrier breakdown using dynamic Gd-DTPA MRI. *Invest. Ophthalmol. Vis. Sci.* 33:3500–3506; 1992.
 15. Tofts, P.S.; Berkowitz, B.; Schnall, M.D. Quantitative analysis of dynamic Gd-DTPA enhancement in breast tumors using a permeability model. *Magn. Reson. Med.* 33:564–568; 1995.
 16. Weinmann, H.J.; Laniado, M.; Mutzel, W. Pharmacokinetics of GdDTPA/Dimeglumine after intravenous injection into healthy volunteers. *Physiol. Chem. Phys. Med. NMR* 16:167–172; 1984.
 17. Tofts, P.S.; Shuter, B.; Pope, J.M. Ni-DTPA doped agarose gel—A phantom material for Gd-DTPA enhancement measurements. *Magn. Reson. Imaging* 11:125–133; 1993.
 18. Tofts, P.S.; Berkowitz, B.A. Rapid measurement of capillary permeability using the early part of the dynamic Gd-DTPA MRI enhancement curve. *J. Magn. Reson. part B* 102:129–136; 1993.
 19. Wehrli, F.W. *Fast-Scan Magnetic Resonance*. 1st ed. New York: Raven Press; 1991: p. 12.
 20. Larsson, H.B.W.; Frederiksen, J.; Kjaer, L.; Henriksen, O.; Olesen, J. In vivo determination of T_1 and T_2 in the brain of patients with severe but stable multiple sclerosis. *Magn. Reson. Med.* 7:43–55; 1988.
 21. Kermode, A.G.; Tofts, P.S.; Thompson, A.J.; MacManus, D.G.; Rudge, P.; Kendall, B.E.; Kingsley, D.P.E.; Moseley, I.F.; du Boulay, E.P.G.H.; McDonald, W.I. Heterogeneity of blood–brain barrier changes in multiple sclerosis: An MRI study with gadolinium-DTPA enhancement. *Neurology* 40:229–235; 1990.
 22. Wang, L.; Lai, H.M.; Lemieux, L.; Tofts, P.S. Detection of disease activity in multiple sclerosis by subtraction of serial image data sets. Nice, France: Society of Magnetic Resonance 3rd meeting; 1995: p. 710.
 23. Tofts, P.S.; Kermode, A.G.; MacManus, D.G.; Robinson, W.H. Nasal orientation device to control head movement during CT and MR studies. *J. Comput. Assist. Tomogr.* 14:163–164; 1990.
 24. MacManus, D.G.; Kermode, A.G.; Tofts, P.S. A repositioning technique for cerebral magnetic resonance imaging of patients with multiple sclerosis. Amsterdam: Society of Magnetic Resonance in Medicine 8th annual meeting; 1989: p. 617.
 25. Hajnal, J.V.; Saeed, N.; Oatridge, A.; Williams, E.J.; Young, I.R.; Bydder, G.M. Detection of subtle brain changes using subvoxel registration and subtraction of serial MR images. *J. Comput. Assist. Tomogr.* 19:677–691; 1995.
 26. Wood, G.K.; Berkowitz, B.A.; Wilson, C.A. Visualization of subtle contrast-related intensity changes using temporal correlation. *Magn. Reson. Imaging* 12:1013–1020; 1994.
 27. Su, M.; Jao, J.; Nalcioglu, O. Measurement of vascular volume fraction and blood–tissue permeability constants with a pharmacokinetic model: Studies in rat muscle tumors with dynamic Gd-DTPA enhanced MRI. *Magn. Reson. Med.* 32:714–724; 1994.
 28. Filippi, M.; Yousry, T.; Campi, A.; Kandziora, C.; Colombo, B.; Voltz, R.; Martinelli, V.; Spuler, S.; Bressi, S.; Scotti, G.; Comi, G. Comparison of triple dose versus standard dose gadolinium-DTPA for detection of MRI enhancing lesions in patients with multiple sclerosis. *Neurology* 46:379–384; 1996.